Published in final edited form as:
J Mol Biol. 2008 December 5; 384(1): 206–218. doi:10.1016/j.jmb.2008.09.022.

Time Evolution of the Quaternary Structure of *Escherichia coli* Aspartate Transcarbamoylase upon Reaction with the Natural Substrates and a Slow Tight Binding Inhibitor

Jay M. West[1], **Jiarong Xia**[1], **Hiro Tsuruta**[2], **Wenyue Guo**[1], **Elizabeth M. O'Day**[1], and **Evan R. Kantrowitz**[1,*]

1*Department of Chemistry, Boston College, Merkert Chemistry Center, Chestnut Hill, MA 02467-3807*

2*Stanford Synchrotron Radiation Laboratory, Stanford Linear Accelerator Center, Stanford University, 2575 Sand Hill Road, MS69, Menlo Park, CA 94025-7015*

Abstract

Here we present a study of the conformational changes of the quaternary structure of *E. coli* aspartate transcarbamoylase (ATCase), as monitored by time-resolved small-angle X-ray scattering (TR-SAXS), upon combining with substrates, substrate analogs, and nucleotide effectors at temperatures between 5 – 22 °C, obviating the need for ethylene glycol. TR-SAXS time courses tracking the T → R structural change after mixing with substrates or substrate analogs appeared to be a single phase under some conditions and biphasic under other conditions, which we ascribe to multiple ligation states producing a time course composed of multiple rates. Increasing the concentration of substrates up to a certain point increased the T → R transition rate, with no further increase in rate beyond that point. Most strikingly after addition of PALA to the enzyme the transition rate was over one order of magnitude slower than with the natural substrates. These results on the homotropic mechanism are consistent with a concerted transition between structural and functional states of either low-affinity low-activity or high-affinity high-activity for aspartate. Addition of ATP along with the substrates increased the rate of the transition from the T to the R state and also decreased the duration of the R-state steady-state phase. Addition of CTP or the combination of CTP/UTP to the substrates significantly decreased the rate of the T → R transition and caused a shift in the enzyme population towards the T state even at saturating substrate concentrations. These results on the heterotropic mechanism suggest a destabilization of the T state by ATP and a destabilization of the R state by CTP and CTP/UTP, consistent with the T and R state crystallographic structures of ATCase in the presence of the heterotropic effectors.

Keywords

cooperativity; quaternary structure; allosteric transition; small-angle X-ray scattering

*Corresponding author. E-mail address: evan.kantrowitz@bc.edu.

Introduction

Aspartate transcarbamoylase (E.C.2.1.3.2, ATCase) catalyzes one of the first steps in pyrimidine nucleotide biosynthesis, the reaction of carbamoyl phosphate (CP), with *L*-aspartate (Asp) to form *N*-carbamoyl-*L*-aspartate and inorganic phosphate (P_i).[1] In many prokaryotes such as *Escherichia coli* this reaction is the committed step in pyrimidine nucleotide biosynthesis. *E. coli* ATCase is composed of two types of subunits. The two larger or catalytic subunits are each composed of three identical polypeptide chains (M_r 34,000), while the three smaller or regulatory subunits are each composed of two identical polypeptide chains (M_r 17,000). Each of the six active sites is located at the interface between two adjacent catalytic chains, and side chains required for catalysis are recruited to the active site from both chains.[2] The enzyme demonstrates homotropic cooperativity for the substrate Asp and is heterotropically regulated by the effectors ATP, CTP,[3] and UTP in the presence of CTP.[4]

The structures of the low-activity T state (in the absence of substrates)[5,6] and high-activity R state (in the presence of substrates or substrate analogues such as N-phosphonacetyl-L-aspartate, PALA)[7–9] have been determined by X-ray crystallography. A comparison of the T and R structures reveals that during the T → R transition, the two catalytic trimers increase their separation along the 3-fold axis by about 11 Å and rotate about 5° around the same axis, while the regulatory dimers rotate about 15° around their respective 2-fold axes.[10] The 11 Å expansion of the enzyme observed during the T → R transition is easily monitored by small-angle X-ray scattering (SAXS).[11] Thus, the SAXS pattern is a sensitive and specific probe to study the quaternary conformational changes of the enzyme.

By using SAXS as a structural probe in stopped-flow experiments, the time-evolution of the quaternary conformational changes of ATCase have been monitored.[12,13] These studies showed that the enzyme when mixed with substrates is very quickly converted from the T to the R state, the enzyme remains in the R state until substrates are exhausted, and then the enzyme reverts back to the T state. These early studies required integration of the signal over time intervals of 100 – 200 ms and averaging over many runs to improve the signal to noise ratio.[12,13] Because of the relatively long time window for each point it was necessary to slow the reaction rate, which was done by performing the reaction at −5° C in a buffer containing 20% ethylene glycol.

Dreyfus *et al.*[14] showed that a variety of alcohols such as methanol, ethanol, 1-propanol, 2-propanol, 1-butanol, and 2-methyl-2-propanol have a significant influence on the activity and homotropic cooperativity of ATCase. For example, 20% methanol or ethanol reduced the activity of ATCase by approximately 90%. Additional studies with 15% ethanol showed a shift in the pH optimum of the reaction and an alteration in the Hill coefficient. Their interpretation of these solvent effects was that the cosolvent preferentially stabilized the T or R state of the enzyme depending upon the relative concentration and polarity of the cosolvent. For the simple alcohols, the primary effect was stabilization of the T state. Although ethylene glycol was not investigated by Dreyfus *et al.*,[14] one would predict that ethylene glycol with its two hydroxyl groups would behave similarly to methanol and ethanol.

Here we reinvestigate the time-evolution of the quaternary conformational changes of ATCase in the absence of ethylene glycol. This was made possible by significant instrumental developments including a fast CCD X-ray detector and a high-flux X-ray beam via a multilayer monochromator[15], with an increase in beam brightness due to the update of the synchrotron storage ring at Stanford Synchrotron Radiation Laboratory (SSRL) to SPEAR3, a third generation source. These improvements allowed the collection of time-resolved SAXS data at a time resolution as short as 5 ms. Using this system we were able to study the quaternary

conformational changes of ATCase in the temperature range of 5–22 °C in the absence of ethylene glycol.

Results

Kinetics of the ATCase reaction in the presence of ethylene glycol

Since previous TR-SAXS experiments were performed in the presence of 20% ethylene glycol,[12,13] and Dreyfus *et al*.[14] showed that a variety of alcohols at concentrations of 20% or less can dramatically alter the catalytic turnover rate and cooperativity of ATCase, kinetic assays were performed in the presence of ethylene glycol to determine if it had any influence on the ATCase reaction. As shown in Figure 1(a), ethylene glycol dramatically reduced the activity of ATCase at 5 °C. In the presence of 20% ethylene glycol the activity of the enzyme was reduced by 75%. In addition to reducing the activity of the enzyme, ethylene glycol had a small influence on homotropic cooperativity (data not shown).

Ethylene glycol also has a significant influence on the ability of the heterotropic effectors to modulate enzyme activity. As shown in Figure 1 (b) at 5 °C the presence of 20% ethylene glycol increased the activation of the enzyme by ATP, while reducing the inhibition by CTP. The maximal activation by ATP increased from 220% to 274% in the presence of 20% ethylene glycol. The residual activity at a saturating concentration of CTP was 29% as compared to 48% in the presence of ethylene glycol. The value of K_{ATP} (K is the nucleotide concentration required at 50% maximal activation or inhibition of the enzyme) increased from 0.47 mM to 0.72 mM in the presence of 20% ethylene glycol. The value of K_{CTP} increased from 7.8 μM to 14.5 μM in the presence of 20% ethylene glycol.

The ability of UTP to act as a synergistic inhibitor of ATCase in the presence of CTP[4] was also tested at 5°C in the absence and presence of 20% ethylene glycol. In the absence of ethylene glycol the combination of 4 mM CTP and 4 mM UTP (CTP/UTP) yielded a residual activity of the enzyme of 22%, whereas in the presence of ethylene glycol the combination of CTP/UTP yielded a residual activity of the enzyme of 28%.

Kinetics of the ATCase reaction at 5 °C

Because the TR-SAXS experiments reported here were performed at temperatures as low as 5 °C, the kinetic properties of ATCase were fully characterized at 5 °C in the same buffers used for the TR-SAXS experiments (Figure 2). As shown in Table 1, many aspects of catalysis at 25 °C are not only quantitatively different at 5 °C, but in some cases qualitatively different. As would be expected, the maximal observed velocity was reduced by nearly 5-fold. This reduction in velocity was accompanied by an almost 3-fold decrease in the concentration of Asp required for half-maximal activity ($[Asp]_{0.5}$), and a decease in the Hill coefficient (n_H) from 2.6 to 2.0. The observed changes in $[Asp]_{0.5}$ and n_H are similar to the changes observed when Asp saturating curves are determined in the presence of ATP, suggesting that, like ATP, lower temperatures shift the equilibrium towards the R state. This phenomenon was demonstrated in a previous SAXS study by the shift in the structural equilibrium of the mutant D236A enzyme in the direction of the R state with decreasing temperature.[16] At 5 °C the $[Asp]_{0.5}$ decreased nearly 2-fold in the presence of ATP; increased 20% in the presence of UTP; increased over 2-fold in the presence of CTP; and increased by a factor of 2.5 in the presence of CTP/UTP. A similar trend was also observed at 25 °C. The $[Asp]_{0.5}$ decreased over 2-fold in the presence of ATP; increased 10% in the presence of UTP; increased nearly 2-fold in the presence of CTP; and increased by 2.3-fold in the presence of CTP/UTP.

The kinetic data at 5 °C was plotted as v/V_{max} *vs*. [Asp] as shown in Figure 3 and fitted by the theoretical curve of $\bar{Y}_{Asp}$ (fraction of active sites occupied by Asp) vs. $\alpha K_{R(Asp)}$, which is

derived from the equations of the theoretical two-state allosteric transition model proposed by Monod *et al*.[17,18]

$$\overline{Y}_{\mathrm{Asp}} = \frac{\alpha(1+\alpha)^{n-1} + L'\alpha c_{\mathrm{Asp}}(1+\alpha c_{\mathrm{Asp}})^{n-1}}{(1+\alpha)^{n} + L'(1+\alpha c_{\mathrm{Asp}})^{n}}$$

where $\alpha = [\mathrm{Asp}] / K_{R(\mathrm{Asp})}$, L' is the allosteric equilibrium constant in the presence of saturating CP, and $c_{\mathrm{Asp}} = K_{R(\mathrm{Asp})} / K_{T(\mathrm{Asp})}$. $K_{T(\mathrm{Asp})}$ and $K_{R(\mathrm{Asp})}$ are the dissociation constants of Asp for the T and R allosteric states, respectively. A value of L' = 10 was obtained from the static SAXS data shown in Figure 4, according to the methods of Tsuruta *et al.*[13] The starting point used for $K_{R(\mathrm{Asp})}$ was the $[\mathrm{Asp}]_{0.5}$ = 5.1 mM value obtained from the kinetic data. After obtaining a suitable fit for the data the values of $K_{R(\mathrm{Asp})}$ = 3.5 ± 0.5 mM and $K_{T(\mathrm{Asp})}$ = 40 ± 10 mM were derived.

Time-Resolved X-ray Scattering: Effect of substrates and substrate analogues

TR-SAXS was used to monitor the quaternary conformational changes that ATCase undergoes when the enzyme is mixed with substrates. Using the high beam flux obtained by the multilayer monochromator and fast CCD detector at SSRL, practical time resolution of the TR-SAXS data collection was improved from 100 – 200 ms[19] to as low as 5 ms in a single mixing event. However, the rate constants for the T → R transition presented here were obtained from 19 ms collection rate data, because at this rate the signal to noise ratio was significantly better and fast enough to record much of the transition. This improvement in detection allowed reactions to be monitored in the temperature range between 5 °C and 22 °C, rather than at −5 °C as previously reported.[19]

Shown in Figure 5 (a) are a series of SAXS patterns recorded upon mixing 1.5 mM ATCase (in active sites) plus 50 mM CP in one syringe with 100 mM Asp plus 50 mM CP in the second syringe at 5 °C. Immediately after mixing the enzyme concentration was 0.75 mM in active sites (37.5 mg/ml), while the CP and Asp concentrations were each 50 mM. The SAXS patterns shown in Figure 5 (a) are at 38 ms, 380 ms, and 3800 ms. The scattering pattern at 38 ms does not correspond to either the T or R states as the enzyme population is in the process of undergoing the quaternary conformational change. The pattern at 380 ms is essentially identical to the curve of the enzyme in the presence of PALA (R state), while the curve at 3800 ms is essentially the same as that observed in the presence of D-Asp and CP (T state). To determine if the curve at 38 ms corresponded to the formation of a transient intermediate on the pathway between the T and R states, a curve was generated from a sum of fractions of the T (33%) and R (67%) state curves corresponding to a value of L = 0.5.[13] This generated curve is a near match to the X-ray scattering curve recorded at t = 38 ms after mixing the enzyme with substrates.

In order to help visualize the time course of structural change, the area under the curves between $s = 0.085$ Å^{-1} and $s = 0.152$ Å^{-1} was integrated and plotted as a function of time. This integration converts observed scattering intensity to relative concentration of the enzyme species on the basis that solution scattering intensity reflects relative concentration of each species linearly, in the absence of oligomeric state changes. Figure 5 (b) shows the time-dependent change in the integrated intensity of the SAXS pattern for this experiment. At t ≅ 5 – 10 ms, (t = 0 as shown on the plot. The dead time of the stopped-flow mixer is approximately 5 – 10 ms) the enzyme population is nearly a equal mixture of T and R state molecules. Between t = 100 ms and t = 1500 ms 95% of the enzyme population is in the R-state as the enzyme catalyzes the reaction converting Asp and CP into carbamoyl aspartate and P_i. After t = 1500 ms the enzyme population is returning to the T state as the substrates are depleted, and after

3000 ms virtually the entire enzyme population is back in the T state. At 5 °C the turnover rate at maximal velocity of the holoenzyme is 350 ± 40 s^{-1}. At a substrate concentration of 50 mM and an active site concentration of 0.75 mM the substrate:holoenzyme ratio is 400, so it should take 1 – 1.3 seconds to consume the substrate. The R-state plateau, defined here as the region of >95% of the peak amplitude of the integrated scattering curve, has a total duration of 1.4 seconds, which demonstrates that enzyme quickly reverts to the T state after depleting the substrates.

When ATCase is mixed with D-Asp and CP, (final concentrations 0.75 mM active sites, [D-Asp] = [CP] = 50 mM) the TR-SAXS curve showed virtually no change (see Figure 5 and Figure 6). The use of D-Asp thus provides a control for the L-Asp experiments with a compound with equal scattering potential or electron density, and as a control for the T-state scattering curve as previously described.[19] The integrated intensity at the end of experiment when L-Asp and CP are mixed was practically identical to that observed when D-Asp and CP are mixed with enzyme. Because the TR-SAXS curve returns to the level observed in the presence of D-Asp and CP, it is clear that virtually the entire enzyme population has reverted back to the T state after the substrates have been depleted.

The initial time-course of the structural change after combining the enzyme with substrates or substrate analogs appeared to fit to either a single or double exponential depending upon the experimental conditions. Therefore each set of data was fit to both exponential fits and the number of rate constants (represented as $k_{T\rightarrow R(1)}$ for the first or fast phase and $k_{T\rightarrow R(2)}$ for the second or slow phase, where applicable) reported reflects which fit was superior. As demonstrated by the rate constant data for the quaternary structural change in Table 2, increasing the substrate concentration from 25 mM to 50 mM and doubling the enzyme concentration increased the rate of the fast phase of the transition from 18.3 s^{-1} to 51 s^{-1}. In this experiment it was necessary to use a lower enzyme concentration at the lower substrate concentration in order to observe the full T to R conversion of the enzyme population before significant depletion of the substrates. Lowering the enzyme concentration by one half, to 18 mg/ml, and half again to, 9 mg/ml, while keeping the substrate concentration at 50 mM did not change the rate of the fast or slow phase, within error, of the T → R transition (data not shown). Therefore an enzyme concentration of 37.5 mg/ml was used for all experiments, with the previous exception, for a superior signal to noise ratio for the scattering data. Increasing the substrate concentration further to 100 mM while maintaining the same enzyme concentration (37.5 mg/ml) did not change the rate of transition for the fast or slow phases, as might be expected since this concentration was much higher than the $[Asp]_{0.5}$ value of 5.1 mM.

In order to establish the value for the integrated intensity and scattering pattern of the R-state structure of ATCase in a TR-SAXS experiment, PALA was mixed with enzyme and CP (final concentrations 0.75 mM active sites, 5 mM PALA, 50 mM CP). As seen in Figure 6, the integrated intensity observed immediately after mixing was shifted towards the R-state value. The rate constants for the fast and slow phases after mixing with PALA were both more than an order of magnitude slower than the corresponding T → R transition rate constants observed in the presence of a saturating concentration of the natural substrates, L-Asp and CP. The single fast phase rate constant for the structural change with 50 mM succinate and 50 mM CP was 38 s^{-1}, similar to the rate of the fast phase with the natural substrates at a saturating concentration.

Effect of Nucleotides

The time-course of the quaternary structural change in the presence of ATP is shown in Figure 7 and is similar to that observed in the absence of nucleotides. However, in the presence of ATP, the duration that the enzyme remains in the R-state plateau is shorter than in the absence of nucleotides and the $k_{T\rightarrow R(1)}$ increased from 51 s^{-1} to 89 s^{-1}. The time-course of the structural

change for ATCase in the presence of the nucleotide inhibitors are shown in Figure 8. The rate of T → R transition in the presence CTP and CTP/UTP decreased significantly, to 12 s^{-1} and 10.3 s^{-1} respectively. The integrated scattering intensity of the R-state plateau in the presence of CTP and CTP/UTP is lower than that observed in the absence of nucleotides, and the duration of the plateau in the presence of CTP and CTP/UTP is much shorter than in the absence of nucleotides.

The results with UTP alone were unexpected. The rate of the fast phase of the T → R transition in the presence of UTP was identical to that in the absence of nucleotides. The integrated scattering intensity of the R-state plateau in the presence of UTP is also the same as in the absence of nucleotides. However, the duration of the R-state plateau phase in the presence of UTP is only half of that observed in the absence of nucleotides, suggesting a slight destabilization of the R state by UTP.

Determination of the Activation Energy of ATCase

The kinetics of the quaternary structural change were observed at a series of temperatures between 5 °C and 22 °C in order to calculate the activation energy of the quaternary conformational changes of ATCase both from the T to the R state and from the R to the T state. Unfortunately, above 10 °C the T → R transition rate is so fast that our instrumentation was unable to follow it. However, the rate constants for the $R_0 \rightarrow T_0$ (unliganded states) transition after the substrates were exhausted were obtained by fitting the lower half of the return phase to a single exponential fit. The rate constants for the $R_0 \rightarrow T_0$ transition ($k_{R \rightarrow T}$) at 5, 10, 16, and 22 °C were 2.08 ± 0.03, 3.7 ± 0.1, 5.1 ± 0.1, and 8.3 ± 0.1 s^{-1} respectively. An Arhennius plot of these data is shown in Figure 9, which yielded an activation energy for the $R_0 \rightarrow T_0$ transition of 13.0 ± 0.4 kcal/mol.

DISCUSSION

TR-SAXS experiments investigating the time-evolution of the quaternary structural change of ATCase induced by the binding of the natural substrates CP and L-Asp were performed here in the absence of ethylene glycol. In previous studies[19] 20% ethylene glycol was added to all solutions to allow the experiment to be performed at −5 °C. Here we demonstrate that ethylene glycol dramatically alters the homotropic and heterotropic kinetics of the enzyme, as is the case with many other alcohols.[14] Therefore these new studies were important not only in monitoring the quaternary structural change at temperatures closer to physiological, but also because ethylene glycol was eliminated from the reaction.

In order to better correlate the time-resolved structural results reported here at 5 °C to the functional characteristics of ATCase at this temperature, a complete kinetic characterization of the enzyme was performed at 5 °C. As would be expected, the maximal velocity of the enzyme at 5 °C in the absence and presence of the nucleotide effectors was reduced nearly five-fold as compared to the maximal velocity at 25 °C. The $[Asp]_{0.5}$ at 5°C in the absence of nucleotides was also reduced nearly 3-fold, with a concomitant reduction in the cooperativity for Asp (see Table 1). Similarly in the presence of nucleotides at 5°C, the $[Asp]_{0.5}$ was reduced but with no change in cooperativity, except when CTP was present, where the cooperativity increased. The results of these kinetic experiments suggest that the structural results obtained from the TR-SAXS experiments performed at 5 °C should strongly correlate with the structure and function of the enzyme at higher temperatures.

In agreement with previous results,[19] when ATCase is mixed with its natural substrates, CP and L-Asp, there is a rapid structural transition of the enzyme from the T to the R state. The preponderance of the enzyme population remains in the R state as the enzyme reacts with the substrates, and then reverts to the T state when the substrates are exhausted (see Figure 5 (b)).

This clearly demonstrates that the allosteric transition is not the rate-limiting step in catalysis, as has been previously suggested.[20] Therefore, under conditions of saturating substrates the enzyme remains in the R-quaternary structure until the substrates are essentially exhausted and then reverts to the T-quaternary structure.

As shown in the inset to Figure 5 (b), the T → R structural transition upon addition of the natural substrates to the enzyme appears to be a biphasic exponential process, with a fast and slow phase. In this particular case the fast phase accounts for approximately 75% of the total amplitude of the curve, representing the change in integrated intensity between the mixture of T and R states at the first recorded time point and R state at the curve plateau. Considering the evidence against the formation of a structural intermediate as demonstrated in Figure 5 (a), along with the structural transition being a single-phase exponential process in the presence of allosteric inhibitors, as shown in Figure 8, we determined that the curve monitoring the structural change may represent a composite of T-state species with different ligation states, each with its own particular rate of transition to the R state, as has been previously suggested in studies of the rate of the structural change in aspartate transcarbamoylase.[13,21] In the case of the allosteric protein hemoglobin, it is well documented that not only different ligation states but also configurational isomers, or asymmetric ligation states, exhibit a wide range of structural transition rates that originate from different activation energies for the structural change.[22,23] When all the CP binding sites of T-state ATCase are saturated, as they are under our experimental conditions, there are thirteen possible species or ligation states with aspartate bound in the six binding sites when taking into account the T-state interactions between the C1 and C4 chains on opposing catalytic trimers. Therefore the two rates we observe are the composites of up to thirteen or more individual rates for the T → R transition when accounting for these configurational isomers. The observed rate of the T → R transition increases about 3-fold when doubling the aspartate concentration from 25 mM, a concentration well in excess of the $K_{R(Asp)}$ value of 3.5 ± 0.5 mM, to 50 mM, while also doubling the enzyme concentration. Therefore, we are confident that the structural transition is triggered by aspartate binding to the T state, and is not a simple shift in the preexisting equilibrium between the T and R states towards the R state caused by aspartate binding only to that state and "locking" it into that state. If the structural transition were simply a population shift to the R state, then the rate would not change or change very little when increasing the aspartate concentration from 25 mM to 50 mM as both concentrations are well in excess of $K_{R(Asp)}$. This can be accounted for using a kinetic version of the two-state model, which would suggest 14 individual rates for the allosteric transition, defining the T to R equilibrium constants at the 7 ligation states.[24] In order to approximate the average number of aspartate molecules bound to the T state during the structural transition, we used the equation derived for the two-state allosteric model of Monod *et al*., simplified by assuming a saturating concentration of CP in the manner previously described to fit our aspartate saturation data at 5 °C.[17,18] After obtaining a reasonable fit of the data and extracting the appropriate parameters, we obtained a $K_{T(Asp)}$ value of 40 ± 10 mM. With an active site concentration of 0.75 mM and an aspartate concentration of 25 mM an average of 33 – 46% of the active sites are ligated with aspartate (2 – 2.5 per holoenzyme). Similarly, at an aspartate concentration of 50 mM an average of 50 – 67% of the active sites are ligated with aspartate (3 – 4 per holoenzyme) and at an aspartate concentration of 100 mM an average of 67 – 77% of the active sites are ligated with aspartate (4 – 4.6 per holoenzyme). These observations compare favorably with the previous SAXS studies of Fetler *et al*.[25] that two PALA molecules per ATCase holoenzyme molecule are necessary to shift the T to R equilibrium in favor of the R state, and four PALA molecules are necessary to shift the entire enzyme population to the R state. Macol *et al*.[26] demonstrated that the binding of one PALA molecule could shift the entire holoenzyme population to the R state, however, the holoenzyme was comprised of five chains with the R105A mutation. In either case the enzyme clearly does not need to be saturated with substrate analogs or presumably substrates, in order to shift the equilibrium towards the R state. Our findings suggest that the faster observed rate is the

composite of rates of the structural transition for the highly liganded species, with three or more active sites filled. Likewise, the slower observed rate may be the composite of structural transition rates of the least liganded species, with two or fewer active sites filled. At an aspartate concentration of 25 mM we observe only one exponential fit to the data, which according to our model would be the composites of rates of the least liganded species along with the rates of the highly liganded species containing three or more aspartate present as a small fraction of the mixed population. Increasing the aspartate concentration from 50 mM to 100 mM yielded identical rates for both observed phases, suggesting that once three or more aspartate molecules are bound to the holoenzyme the rate for the structural transition is near a maximum, or that highly liganded T-state molecules bound with four or more aspartate are present as only a small fraction of the population even at high aspartate concentrations. Further evidence for this model is provided by comparison of the ratio of the fast phase amplitude to the slow phase amplitude at 50 mM aspartate and 100 mM aspartate concentrations; at the higher aspartate concentration the ratio is higher, suggesting a shift in population towards the highly liganded molecules.

There are some substantial qualitative differences between these TR-SAXS results and the data obtained previously in the presence of ethylene glycol,[19] such as the time-course of the TR-SAXS pattern of the enzyme in the presence of ATP, shown in Figure 7. We observed that the R-state plateau region in the presence of ATP, during which most of the substrates are being converted to products, is shorter than in the absence of ATP. This was not unexpected since ATP, an activator of the enzyme, at 5 °C increased the V_{max} value from 4.2 mmol•h^{-1}•mg^{-1} to 5.4 mmol•h^{-1}•mg^{-1} (Table 1) and also the apparent binding affinity of L-Asp, as the $[Asp]_{0.5}$ value decreased from 5.1 mM to 2.9 mM. However, in the presence of 20% ethylene glycol, a longer R-state plateau was observed in the presence of ATP than in its absence.[19] To explain this it was proposed that ATP, in addition to being an activator may possibly become an inhibitor by "increasing the chance of making L-Asp bind to the active site before P_i leaves and locking the active site into an unproductive cycle with no alteration of the quaternary structure".[19] In that experiment the activity of enzyme was dramatically reduced not only by the presence of 20% ethylene glycol, which as demonstrated in Figure 1(a) reduces the activity by 75%, but also by performing the TR-SAXS at −5 °C. The similar phenomenon of "substrate inhibition" has been observed for the isolated catalytic subunit and for the incomplete complexes C_6R_4 and C_3R_6, as well as for the holoenzyme C_6R_6,[27–29] where a high aspartate concentration ostensibly acts as an inhibitor by binding to the CP binding site.

As detailed in Table 2, ATP increased the rate of the T → R transition, specifically the rate of the fast phase, by approximately 75%. It should be noted that in the presence of ATP the allosteric transition is so rapid that with the current instrumentation the experimental error is somewhat large. As discussed previously, saturating the enzyme with aspartate beyond a concentration of 50 mM did not increase the rate of the structural transition. Therefore one possible interpretation is that ATP increases the on rate of aspartate to the T state,[20] suggesting that aspartate binding is a rate-limiting step in the allosteric transition. However, a more elegant explanation, which is in accord with the data from the inhibitors CTP and CTP/UTP and numerous studies on the effects of the heterotropic nucleotides,[30–32] can be derived using some aspects of the two-state model of Monod *et al*.[17,18] At pH 7.0 Howlett *et al*.[17,31] observed that ATP increases the stability of the R state relative to the T state by 0.8 kcal and reduces the T to R equilibrium constant from 250 to 7 in the absence of substrates. The R to T transition rate with ATP was reduced by only approximately 15% (Figure 7), suggesting a slight stabilization of the R state, so therefore the large increase in the T → R rate would suggest a significant T state destabilization by ATP. Here the two-state model suggests that ATP binds more tightly to the R state and therefore shifts the structural equilibrium in favor of the R state.[17,31] However, our observation of a possibly different mechanism for ATP was suggested by the crystal structures of the T and R states of the enzyme in the presence of ATP; the T state structure showed a slight shift towards the R state with ATP present,[5] whereas globally the R

state structure was unchanged in the presence of ATP.[33] It should be noted that under these conditions with ATP the V_{max} did increase even though the structural state at saturating substrate levels appears to be the same R state as with no ATP present, with the caveat that the V_{max} value is difficult to obtain precisely from steady-state kinetics curves which exhibit substrate inhibition. This suggests that the previously observed increase in the Asp to CA exchange rate with ATP may influence the catalytic mechanism to a modest degree.[20] However our time-resolved structural study indicates that perturbation of T to R equilibrium specifically via T-state destabilization may be the most significant mechanism of ATP activation of ATCase.

The time-courses of the quaternary structural change in the presence of CTP or CTP/UTP are similar in the presence and absence of ethylene glycol (see Figure 8). For both cases, in the presence of CTP or CTP/UTP the duration of the R-state shifted plateau is shorter and the integrated intensity of the plateau is lower than in the absence of nucleotides, and the observed return to the T-state quaternary structure is a slow exponential decline as the remaining substrates are consumed as the enzyme population shifts towards the T state. The integrated intensity of the peak with CTP present and with CTP/UTP present was approximately 80% and 75% respectively of that when no nucleotides were present, indicative that the percent of high-activity R-state molecules at a saturating substrate concentration was reduced to a likewise value. This is in excellent agreement with the enzymatic kinetic data, in which the V_{max} was, within error, reduced by the same amount as the integrated scattering peak in the presence of CTP and CTP/UTP as compared to when no nucleotides were present. These allosteric inhibitors also reduced the rate of the structural transition by over 4-fold. Similar to the condition when no nucleotides were present and the substrate concentration was 25 mM, the initial time-course of the structural change fits to a single exponential. This suggests that the least liganded species have a rate that is so reduced that we do not observe them before the shortened plateau starts its reversion towards the T state, or that the R → T rate for these species is nearly equal to the T → R transition rate. As with the case of ATP, our experimental observations are not in complete agreement with some of the tenets of the two-state model; the much reduced T → R transition rate suggests the nucleotide inhibitors stabilize the T state, and the incomplete conversion of the enzyme population to the R state at a saturating substrate concentration and shift in equilibrium towards the T state long before the substrates are exhausted caused by the collective R → T rates becoming greater than the T → R rates suggest that they destabilize the R state. Using the two-state model as a theoretical framework, Howlett *et al.*[17,31] observed that CTP increases the stability of the T state relative to the R state by 0.9 kcal and increases the T to R equilibrium constant from 250 to 1250 in the absence of substrates. In addition, the two-state model suggests that CTP (and UTP) exert their influence by binding more tightly to the T state and shifting the structural equilibrium in favor of the T state. However, again as with ATP our observations are somewhat at variance with this model, but are supported by the crystal structures of the T and R states of the enzyme in the presence of CTP; the T state structure globally was unchanged in the presence of CTP,[5] and R state structure was shifted slightly in the direction of the T state with CTP present.[33]

In the case of UTP, by itself it had no influence on the kinetics of the enzyme with the exception of raising the $[Asp]_{0.5}$ slightly. It also had no influence on the kinetics of the T → R transition, except for increasing the rate of the slow phase for reasons that are unclear. However, UTP did have a noticeable effect on the length of time the enzyme spent in the R-state plateau region, causing the enzyme population to begin reverting to the T state before the substrates were exhausted. This indicates that UTP may slightly destabilize the R state, but otherwise does not have an appreciable effect on the allosteric behavior of ATCase under these conditions.

The activation energy of the R → T transition was determined by fitting the bottom half of the return curve, after the enzyme had exhausted the substrates, to a single exponential rate, as

opposed to the upper half of the curve where presumably not all enzyme molecules have completely exhausted the substrate bound to the active sites. By fitting the bottom half of the return curve mainly the rate of $R_0 \rightarrow T_0$ should be observed, which is supported by the very low error in the $k_{R\rightarrow T}$ values obtained. As shown in Figure 9, the $E_{aR\rightarrow T}$ was calculated to be 13.0 ± 1.4 kcal/mol from the slope of the Arrhenius plot. At temperatures above 10 °C the T → R rate was so rapid that the data could not give rates with a reasonable error. Moreover these rates are composites of the multiple species with different ligation states, making interpretation of a single activation energy value problematic. However by making some assumptions, an approximate value for the T → R activation energy was derived for the unliganded T and R states. Assuming that the respective transition states in both the T → R transition and R → T transition are the same, and the free energy difference between the T and R states is 3.3 kcal/mol,[17,31] then the activation energy for the T → R transition should be in the range of 15–18 kcal/mol. The charged-charged hydrogen bonds between Glu239 and Lys164 and non-charged hydrogen bonds between Glu239 and Tyr165 are critical for the stabilization of both the T and R state conformations of the enzyme, which are interchain in the T state and intrachain in the R state.[7] Sakash *et al.*[34] showed that three of the six stabilizing interactions between catalytic chains on opposing subunits involving Glu239 are sufficient to stabilize the enzyme in the T state conformation. Thus at least three of the hydrogen bonds involving Glu239 must be broken during the allosteric transition. Considering a typical charged-charged hydrogen bond energy is approximately 4 kcal/mol and a non-charged hydrogen bond energy is approximately 0.5 – 1.5 kcal/mol,[35,36] the minimal energy required for the allosteric transition of the enzyme is 13.5 – 16.5 kcal/mol. The results reported here are consistent with these calculations.

The rate of the allosteric transition was also measured when ATCase is mixed with two substrate analogs; succinate, an aspartate analog that promotes the T → R state transition when combined with CP, and PALA, a bisubstrate analog that binds at nanomolar affinity and also causes the T → R state transition. The structural transition rate with succinate and CP at a concentration of 50 mM each was slightly lower than the rate with the natural substrates at equivalent concentration and was observed to be a single exponential process. This may be because succinate binds approximately one order of magnitude more tightly than aspartate[17,37,38] and therefore the bulk of the T state molecules should be highly liganded during the transition to the R state. However the structural transition rate with PALA was over one order of magnitude slower than with the natural substrates. The kinetics of the interaction of PALA with the isolated catalytic subunit at pH 7.0 and 25 °C has been studied using stopped flow kinetics and ^{31}P saturation transfer NMR by Cohen and Schachman.[39] They observed a rapid binding of PALA followed by a much slower isomerization of the complex with a forward rate constant of 0.18 s^{-1}, similar to the rate constant of the slow phase we observed by TR-SAXS of 0.31 s^{-1}. However, the catalytic subunit by itself does not undergo a T → R transition so it is unclear whether the similarity of these values implies a similar mechanism between the change in the tertiary structure following PALA binding to the catalytic subunit and change in quaternary structure following PALA binding to the holoenzyme. The rate constant data and integrated scattering intensity presented here were obtained after mixing PALA with enzyme premixed with CP, to be consistent with the other experimental conditions. In addition experiments were performed where PALA was mixed with only the enzyme and the rate constants for the T → R transition were essentially identical (data not shown), which suggests the slow allosteric transition after PALA binding is not caused by having to displace CP from the active site. Because PALA combines elements of both substrates into one covalently linked bisubstrate analog, when the CP moiety of PALA initially binds the aspartate moiety may not be able to bind well to the aspartate binding site with the domains open, as they are in the T state. Subsequently the enzyme may undergo a slow conformational change in order for the aspartate moiety to bind tightly and then complete the T → R structural conversion. In this regard PALA appears to fit in the category of a slow tight-binding inhibitor.[40] However the phenomenon of PALA being a very tight binding bisubstrate analog that causes an initial

conformational change followed by a much slower conformational change needs further investigation to be better understood.

In summary, our data showed ethylene glycol had a profound influence on the kinetics and behavior of ATCase, so therefore the time-evolution of the allosteric transition of ATCase was reinvestigated in the absence of ethylene glycol by SAXS revealing several important new insights. Experimentally, these studies demonstrate that SAXS is now capable of monitoring relatively rapid structural changes at temperatures approaching physiological. The allosteric transition is not the rate-limiting step in ATCase catalysis, and the rate of allosteric transition is increased with increasing substrate concentration up to 50 mM. ATP appears to destabilize the T state and have little effect on the R state. CTP and the combination of CTP/UTP appear to destabilize the R state and stabilize the T state. PALA causes a very slow conformational change as compared to the natural substrates. In the future, novel TR-SAXS experiments could be performed with hybrid ATCase molecules that bind one, two, three, four, or five aspartate molecules to determine the individual rate constants and activation energies for each one of these species. Such studies will be facilitated by further instrumental upgrades that are being made to improve time-resolution. We believe we have begun to arrive at a clear understanding of the allosteric mechanism of ATCase, and further studies into its dynamic behavior utilizing such time-resolved techniques as employed here will be invaluable in this.

EXPERIMENTAL PROCEDURES

Materials

ATP, CTP, UTP, carbamoyl phosphate (CP), L-aspartate, D-aspartate, *N*-carbamoyl-L-aspartate, potassium dihydrogen phosphate, sodium azide, succinate and uracil were obtained from Sigma Chemical Co. (St. Louis, Missouri). Ammonium sulfate, electrophoresis grade acrylamide and trishydroxymethylaminomethane (Tris) were purchased from ICN (Costa Mesa, California). N-phosphonacetyl-L-aspartate (PALA) was obtained from the NCI, National Institutes of Heath. All commercially available starting materials and solvents were reagent grade or better and used without further purification. Carbamoyl phosphate dilithium salt, was purified before use by precipitation from 50% (v/v) ethanol and was stored desiccated at −20°C.

Enzyme preparation

The *E. coli* ATCase was overexpressed utilizing *E. coli*strain EK1104[41] containing plasmid pEK152.[42] The isolation and purification were as described previously.[41] The purity of the enzyme was checked by SDS-PAGE[43] and nondenaturing PAGE.[44,45] The concentration of wild-type enzyme was determined by absorbance measurements at 280 nm with an extinction coefficient of 0.59 cm^2/mg.[46]

The purified enzyme was dialyzed into a buffer solution containing 50 mM Tris, 2 mM DTT pH 8.3 and concentrated to approximately 75 mg/ml. The pH of the buffer solution was readjusted to be approximately 8.3 at 5 °C.

Enzyme Kinetics

The activity of the enzyme was measured by the colorimetric[47] method at either 5 °C or 25 °C. Colorimetric assays were performed at a pH of 8.3, in 50 mM Tris acetate buffer. All of the saturation kinetics were performed in duplicate, and the data points shown are the average values. Data analysis for the steady-state kinetics was carried out as previously described.[48] The experimental data was fit to theoretical equations using non-linear regression. When significant substrate inhibition was present the data was analyzed using an extension of the

Hill equation that includes a term for substrate inhibition [28]. The nucleotide saturation curves were fit to a hyperbolic binding isotherm by non-linear regression.

Small-Angle X-ray Scattering

Time-resolved X-ray scattering experiments were performed on Beam Line 4-2 at Stanford Synchrotron Radiation Laboratory, Menlo Park, CA. Synchrotron radiation from a 20-pole 2 Tesla wiggler was focused by a bent cylinder mirror and monochromatized (X-ray wavelength 1.38 Å) by a pair of synthetic W/B_4C multi-layer diffraction elements[15]. A stopped-flow mixer injected 0.1 ml of enzyme solution and an equal volume of another solution, typically containing substrates or substrate analogs, into an observation cell via a mixing chamber. The observation cell was kept at a constant temperature within an error of ± 0.5 °C. The dead time of our stopped-flow apparatus for X-ray scattering is approximately 5 – 10 ms, which is the earliest time-point that one can obtain after initiation of the enzyme reaction. All stopped-flow experiments were performed at a pH of 8.3, in 50 mM Tris acetate buffer containing 2 mM DTT. The time-resolved measurements were done by mixing solutions from two syringes; one syringe containing the substrate CP, nucleotides where applicable, and enzyme; the second syringe contained the substrates CP and L-Asp (or substrate analogs where applicable) and nucleotides where applicable. D-Asp was substituted for L-Asp for recording the T-state scattering curves without enzyme catalysis as well as for the background correction with identical electron density contrast.

A series of successive measurements of 2D scattering data and corresponding beam intensities were synchronized with the completion of sample mixing. The data sampling rate for all experiments was 19 ms with the exception of the curves displayed in Figure 5, in which the rate was 36 ms. The scattering data were recorded by an image-intensified interline CCD X-ray detector system (Hamamatsu Photonics C4880-80-14A & V5445P),[49] located at ~85 cm from the observation cell. The beam intensities incident on the sample were integrated during a series of CCD exposures by the EMBL data collection system.[49] The detector channel numbers were converted to $s = 2\sin\theta/\lambda$, where 2θ is the scattering angle and λ is the X-ray wavelength (1.38 Å), by recording the position of the (100) and related reflections of a cholesterol myristate powder sample placed at the sample position. Image distortion correction of 2D data was performed using the program Fit2D.[50] Radial integration, intensity scaling, background subtraction and correction for non-uniformity of detector response were done by MarParse, developed at SSRL.[51]

Each reported set of T → R rate constants was obtained from averaging three individual runs under the same conditions, with each run inspected for consistency and any experimental anomalies. The time-courses of the initial quaternary structural change were subject to both one exponential curve fits and two exponential curve fits with terms for separate amplitudes and time constants. The number of reported rate constants reflect which least squares fit yielded the highest R value (correlation coefficient) or goodness of fit under each experimental condition. The time-evolution of the structural change displayed in the Figure 4, Figure 5, Figure 6, and Figure 7 are from individual single-mixing runs and the reported R → T rate constants were obtained from the same individual runs.

Abbreviations used

ATCase, aspartate transcarbamoylase (EC 2.1.3.2, aspartate carbamoyltransferase); CA, carbamoyl aspartate; CP, carbamoyl phosphate; PALA, N-phosphonacetyl-L-aspartate; TR-SAXS, time-resolved small-angle X-ray scattering; 80's loop, a loop in the catalytic chain of aspartate transcarbamoylase comprised of residues 73–88; 240's loop, a loop in the catalytic chain of aspartate transcarbamoylase comprised of residues 230–245.

Acknowledgements

This work was supported in part by Grant GM26237 from the National Institutes of Health. The Stanford Synchrotron Radiation Laboratory (SSRL) is operated by the Department of Energy, Office of Basic Energy Sciences. The SSRL Structural Biology Resource is supported by the National Institutes of Health, National Center for Research Resources (P41RR01209), and by the Department of Energy, Office of Biological and Environmental Research. The content is solely the responsibility of the authors and does not necessarily reflect the official views of NCRR or NIH.

References

1. Reichard P, Hanshoff G. Aspartate carbamyl transferase from *Escherichia coli*. Acta Chem. Scand 1956;10:548–560.
2. Wente SR, Schachman HK. Shared active sites in oligomeric enzymes: Model studies with defective mutants of aspartate transcarbamoylase produced by site-directed mutagenesis. Proc. Natl. Acad. Sci. U.S.A 1987;84:31–35. [PubMed: 3540957]
3. Gerhart JC, Pardee AB. The effect of the feedback Inhibitor CTP, on subunit interactions in aspartate transcarbamylase. Cold Spring Harbor Symp. Quant. Biol 1963;28:491–496.
4. Wild JR, Loughrey-Chen SJ, Corder TS. In the presence of CTP, UTP becomes an allosteric inhibitor of aspartate transcarbamylase. Proc. Natl. Acad. Sci. U.S.A 1989;86:46–50. [PubMed: 2643106]
5. Stevens RC, Gouaux JE, Lipscomb WN. Structural consequences of effector binding to the T state of aspartate carbamoyltransferase: Crystal structures of the unligated and ATP- and CTP-complexed enzymes at 2.6 Å Resolution. Biochemistry 1990;29:7691–7701. [PubMed: 2271528]
6. Wang J, Stieglitz KA, Cardia JP, Kantrowitz ER. Structural basis for ordered substrate binding and cooperativity in aspartate transcarbamoylase. Proc. Natl. Acad. Sci. U. S. A 2005;102:8881–8886. [PubMed: 15951418]
7. Krause KL, Voltz KW, Lipscomb WN. 2.5 Å structure of aspartate carbamoyltransferase complexed with the bisubstrate analog N-(phosphonacetyl)-L-aspartate. J. Mol. Biol 1987;193:527–553. [PubMed: 3586030]
8. Ke H-M, Lipscomb WN, Cho Y, Honzatko RB. Complex of N-phosphonacetyl-L-aspartate with aspartate carbamoyltransferase: X-ray refinement, analysis of conformational changes and catalytic and allosteric mechanisms. J. Mol. Biol 1988;204:725–747. [PubMed: 3066911]
9. Jin L, Stec B, Lipscomb WN, Kantrowitz ER. Insights into the mechanism of catalysis and heterotropic regulation of *E. coli* aspartate transcarbamoylase based upon a structure of enzyme complexed with the bisubstrate analog N-phosphonacetyl-L-aspartate at 2.1 Å. Proteins: Struct. Funct. Genet 1999;37:729–742. [PubMed: 10651286]
10. Lipscomb WN. Aspartate Transcarbamoylase from *Escherichia coli*: Activity and Regulation. Adv. Enzymol 1994;68:67–151. [PubMed: 8154326]
11. Hervé G, Moody MF, Tauc P, Vachette P, Jones PT. Quaternary structure changes in aspartate transcarbamylase studied by X-ray solution scattering; signal transmission following effector binding. J. Mol. Biol 1985;185:189–199. [PubMed: 3900420]
12. Tsuruta H, Sano T, Vachette P, Tauc P, Moody MF, Wakabayashi K, Amemiya Y, Kimura K, Kihara H. Structural kinetics of the allosteric transition of aspartate transcarbamoylase produced by physiological substrates. FEBS Lett 1990;263:66–68. [PubMed: 2185037]
13. Tsuruta H, Vachette P, Sano T, Moody MF, Tauc P, Amemiya Y, Wakabayashi K, Kihara H. Kinetics of the Quaternary Structure Change of Aspartate Transcarbamoylase Triggered by Succinate, a Competitive Inhibitor. Biochemistry 1994;33:10007–10012. [PubMed: 8060968]
14. Dreyfus M, Fries J, Tauc P, Hervé G. Solvent Effects on Allosteric Equilibria: Stabilization of T and R Conformations of *Escherichia coli* Aspartate Trancarbamylase by Organic Solvants. Biochemistry 1984;23:4852–4859. [PubMed: 6388636]
15. Tsuruta H, Brennan S, Rek ZU, Irving TC. A wide-bandpass multilayer monochromator for biological small-angle scattering and fiber diffraction studies. J. Appl. Crystallogr 1998;31:672–682.
16. Fetler L, Kantrowitz ER, Vachette P. Direct observation in solution of pre-existing structure equilibrium for a mutant of allosteric aspartate transcarbamoylase. Proc.Natl. Acad. Sci. U. S. A 2007;104:495–500. [PubMed: 17202260]

17. Howlett GJ, Blackburn MN, Compton JG, Schachman HK. Allosteric regulation of aspartate transcarbamoylase. Analysis of the structural and functional behavior in terms of a two-state model. Biochemistry 1977;16:5091–5099. [PubMed: 334257]
18. Monod J, Wyman J, Changeux JP. On the Nature of Allosteric Transitions: A Plausible Model. J. Mol. Biol 1965;12:88–118. [PubMed: 14343300]
19. Tsuruta H, Kihara H, Sano T, Amemiya Y, Vachette P. Influence of nucleotide effectors on the kinetics of the quaternary structure transition of allosteric aspartate transcarbamylase. J. Mol. Biol 2005;348:195–204. [PubMed: 15808863]
20. Hsuanyu Y, Wedler FC. Effectors of *Escherichia coli* aspartate transcarbamoylase differentially perturb aspartate binding rather than the T-R transition. J. Biol. Chem 1988;263:4172–4181. [PubMed: 3279030]
21. Eckfeldt J, Hammes GG, Mohr SC, Wu CW. Relaxation spectra of aspartate transcarbamylase. I. Interaction of 5-bromocytidine triphosphate with native enzyme and regulatory subunit. Biochemistry 1970;9:3353–3362. [PubMed: 4941833]
22. Eaton WA, Henry ER, Hofrichter J. Application of linear free energy relations to protein conformational changes: the quaternary structural change of hemoglobin. Proc. Natl. Acad. Sci. U. S. A 1991;88:4472–4475. [PubMed: 2034685]
23. Ackers GK, Doyle ML, Myers D, Daugherty MA. Molecular code for cooperativity in hemoglobin. Science 1992;255:54–63. [PubMed: 1553532]
24. Eaton WA, Henry ER, Hofrichter J, Mozzarelli A. Is cooperative oxygen binding by hemoglobin really understood? Nature Struct. Biol 1999;6:351–358. [PubMed: 10201404]
25. Fetler L, Tauc P, Hervé G, Moody MF, Vachette P. X-ray scattering titration of the quaternary structure transition of aspartate transcarbamylase with a bisubstrate analogue: influence of nucleotide effectors. J. Mol. Biol 1995;251:243–255. [PubMed: 7643401]
26. Macol CP, Tsuruta H, Stec B, Kantrowitz ER. Direct structural evidence for a concerted allosteric transition in *Escherichia coli* aspartate transcarbamoylase. Nat. Struc. Biol 2001;8:423–426.
27. Porter RW, Modebe MO, Stark GR. Aspartate transcarbamylase: Kinetic studies of the catalytic subunit. J. Biol. Chem 1969;244:1846–1859. [PubMed: 4889008]
28. Pastra-Landis SC, Evans DR, Lipscomb WN. The Effect of pH on the Cooperative Behavior of Aspartate Transcarbamylase from *Escherichia coli*. J. Biol. Chem 1978;253:4624–4630. [PubMed: 26686]
29. Evans DR, Pastra-Landis SC, Lipscomb WN. Isolation and properties of a species produced by the partial dissociation of aspartate transcarbamylase from Escherichia coli. J. Biol. Chem 1975;250:3571–3583. [PubMed: 1092675]
30. Eisenstein E, Markby DW, Schachman HK. Heterotropic effectors promote a global conformational change in aspartate transcarbamoylase. Biochemistry 1990;29:3724–3731. [PubMed: 2187530]
31. Schachman HK. Can a simple model account for the allosteric transition of aspartate transcarbamylase. J. Biol. Chem 1988;263:18583–18586. [PubMed: 3058687]
32. Velyvis A, Yang YR, Schachman HK, Kay LE. A solution NMR study showing that active site ligands and nucleotides directly perturb the allosteric equilibrium in aspartate transcarbamoylase. Proc. Natl. Acad. Sci. U. S. A 2007;104:8815–8820. [PubMed: 17502625]
33. Gouaux JE, Stevens RC, Lipscomb WN. Crystal structures of aspartate carbamoyltransferase ligated with phosphonoacetamide, malonate and CTP or ATP at 2.8 Å resolution and neutral pH. Biochemistry 1990;29:7702–7715. [PubMed: 2271529]
34. Sakash JB, Chan RS, Tsuruta H, Kantrowitz ER. Three of the six possible intersubunit stabilizing interactions involving Glu239 are sufficient for restoration of the homotropic and heterotropic properties of *Escherichia coli* aspartate transcarbamoylase. J. Biol. Chem 2000;275:752–758. [PubMed: 10625604]
35. Street IP, Armstrong CR, Withers SG. Hydrogen bonding and specificity. Fluorodeoxy sugars as probes of hydrogen bonding in the glycogen phosphorylase-glucose complex. Biochemistry 1986;25:6021–6027. [PubMed: 3790503]
36. Fersht A. The hydrogen bonding in molecular recognition. TIBS 1987;12:301–304.

37. Changeux J-P, Gerhart JC, Schachman HK. Allosteric Interactions in Aspartate Transcarbamoylase: Binding of Specific Ligands to the Native Enzyme and Isolated Subunits. Biochemistry 1968;7:531–538. [PubMed: 4868539]
38. Changeux J, Rubin M. Allosteric interactions in aspartate transcarbamylase. 3. Interpretation of experimental data in terms of the model of Monod, Wyman, and Changeux. Biochemistry 1968;7:553–561. [PubMed: 4868541]
39. Cohen RE, Schachman HK. Kinetics of the interaction of N-(phosphonacetyl)-L-aspartate with the catalytic subunit of aspartate transcarbamoylase. J. Biol. Chem 1986;261:2623–2631. [PubMed: 3949739]
40. Szedlacsek SE, Duggleby RG. Kinetics of slow and tight-binding inhibitors. Methods Enzymol 1995;249:144–180. [PubMed: 7791610]
41. Nowlan SF, Kantrowitz ER. Superproduction and rapid purification of *E. coli* aspartate transcarbamoylase and its catalytic subunit under extreme derepression of the pyrimidine pathway. J. Biol. Chem 1985;260:14712–14716. [PubMed: 3902838]
42. Baker DP, Kantrowitz ER. The conserved residues glutamate-37, aspartate-100 and arginine-269 are important for the structural stabilization of *Escherichia coli* aspartate transcarbamoylase. Biochemistry 1993;32:10150–10158. [PubMed: 8104480]
43. Laemmli UK. Cleavage of structural proteins during the assembly of the head of bacteriophage T4. Nature 1970;227:680–685. [PubMed: 5432063]
44. Davis BJ. Disc electrophoresis-II Method and application to human serum proteins. Ann. N.Y. Acad. Sci 1964;121:404–427. [PubMed: 14240539]
45. Ornstein L. Disc electrophoresis. I. Background and theory. Ann. N.Y. Acad. Sci 1964;121:321–349. [PubMed: 14240533]
46. Gerhart JC, Holoubek H. The purification of aspartate transcarbamylase of *Escherichia coli*and separation of its protein subunits. J. Biol. Chem 1967;242:2886–2892. [PubMed: 5338508]
47. Pastra-Landis SC, Foote J, Kantrowitz ER. An improved colorimetric assay for aspartate and ornithine transcarbamylases. Anal. Biochem 1981;118:358–363. [PubMed: 7337232]
48. Silver RS, Daigneault JP, Teague PD, Kantrowitz ER. Analysis of two purified mutants of *Escherichia coli* aspartate transcarbamylase with single amino acid substitutions. J. Mol. Biol 1983;168:729–745. [PubMed: 6350607]
49. Boulin CJ, Dainton D, Dorrington E, Elsner G, Gabriel A, Bordas J, Koch MHJ. Systems for time resolved x-ray measurements using one-dimensional and two-dimensional detectors - Requirements and pratical experience. Nuc. Instru. Meth. Phys. Res 1982;201:209–220.
50. Hammersley AP, Svensson SO, Thompson A, Graafsma H, Kvick A, Moy JP. Calibration and correction of distortions in 2-dimensional detector systems. Rev. Sci. Instru 1995;66:2729–2733.
51. Smolsky IL LP, Niebuhr M, Ito K, Weiss TM, Tsuruta H. Biological small-angle x-ray scattering facility at the Stanford Synchrotron Radiation Laboratory. J. Appl. Cryst 2007;40:S453–S458.

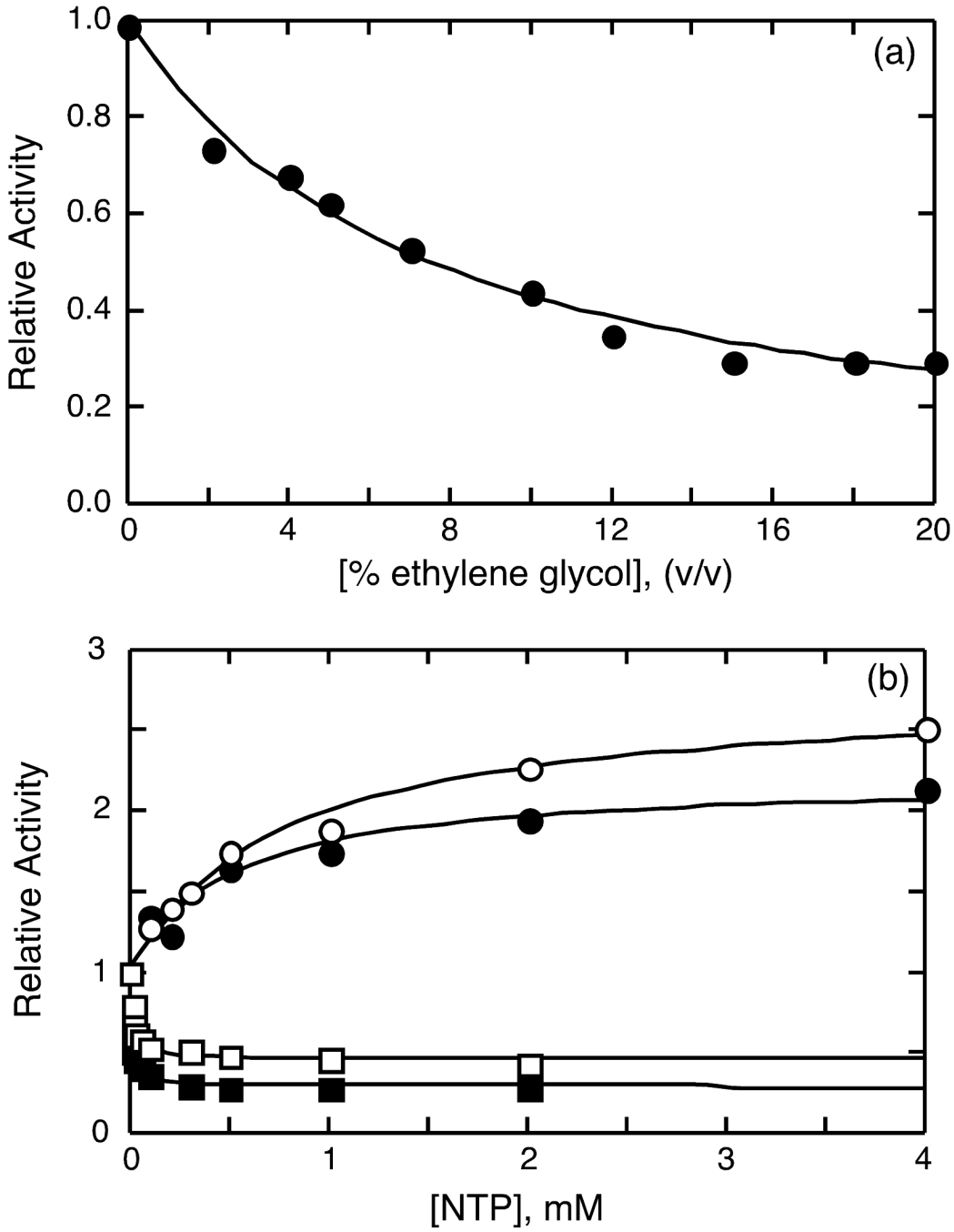

Figure 1.

(a) The dependence of activity of ATCase on the concentration of ethylene glycol. All measurements were made at 5° C in the presence of 50 mM Tris, 2 mM DTT, pH 8.3. (b) Influence of the nucleotide effectors ATP and CTP on the activity of ATCase in the presence and absence of 20% ethylene glycol. Colorimetric assays were performed at 5° C in 50 mM Tris acetate buffer (pH 8.3) at a subsaturating concentration of L-Asp (2.4 mM) and saturating CP concentration (4.8 mM), in the presence of ATP and 20% ethylene glycol (v/v) (○), in the presence of ATP and in the absence of ethylene glycol (●), in the presence of CTP and 20% ethylene glycol (v/v) (□), in the presence of CTP and in the absence of ethylene glycol (v/v) (■).

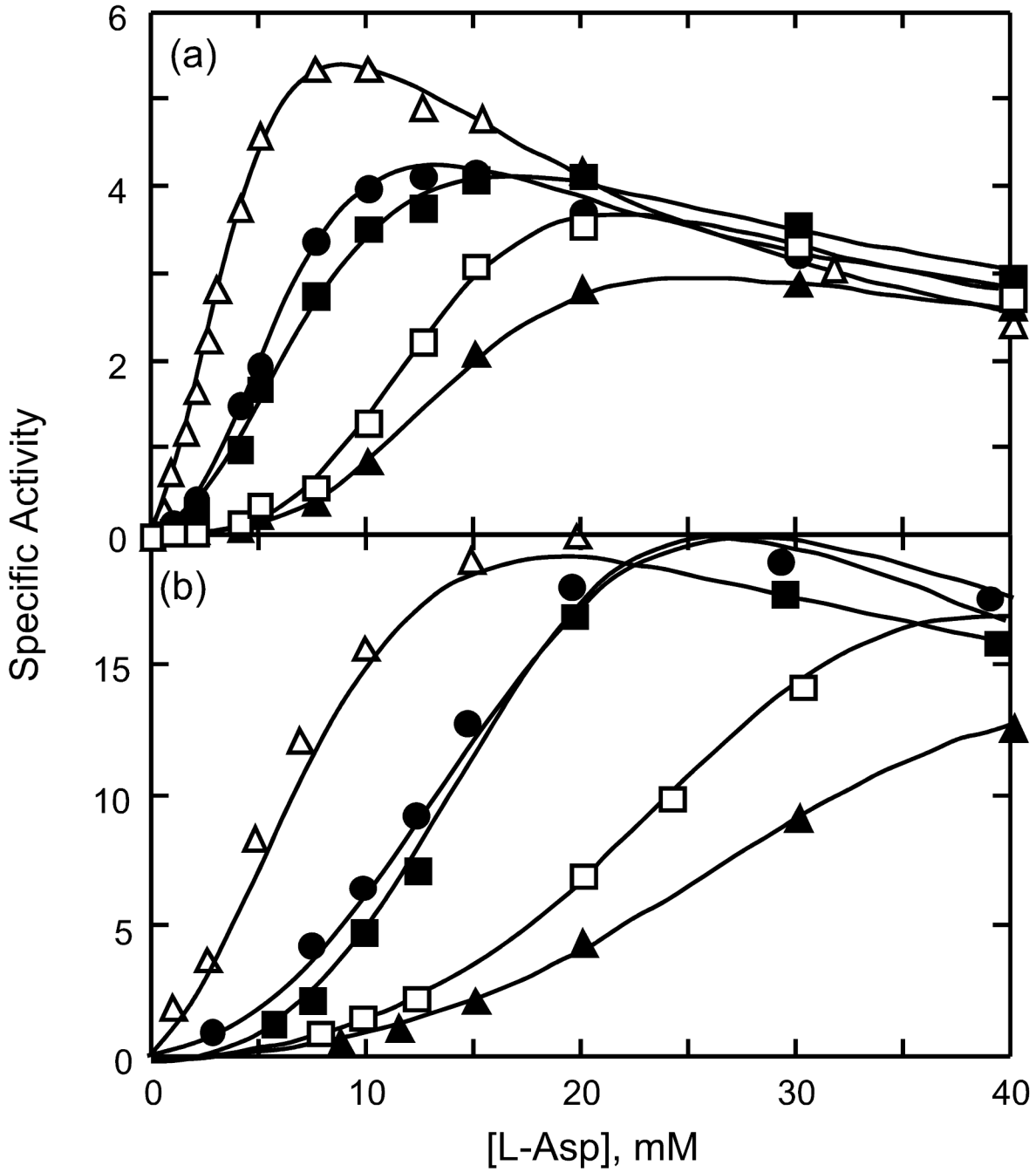

Figure 2.

L-Asp saturation kinetics in the absence and presence of the nucleotide effectors at (a) 5° C and (b) 25 °C. Reactions were carried out in 50 mM Tris buffer, pH 8.3. The kinetic curves were determined in the presence of 5 mM ATP (Δ), 4 mM CTP (□), 4 mM UTP (■), 4 mM CTP and 4mM UTP (▲) as compared to the saturation kinetics in the absence of nucleotide (●). Specific activity is reported in units of mmoles of carbamoyl aspartate formed per mg per hr.

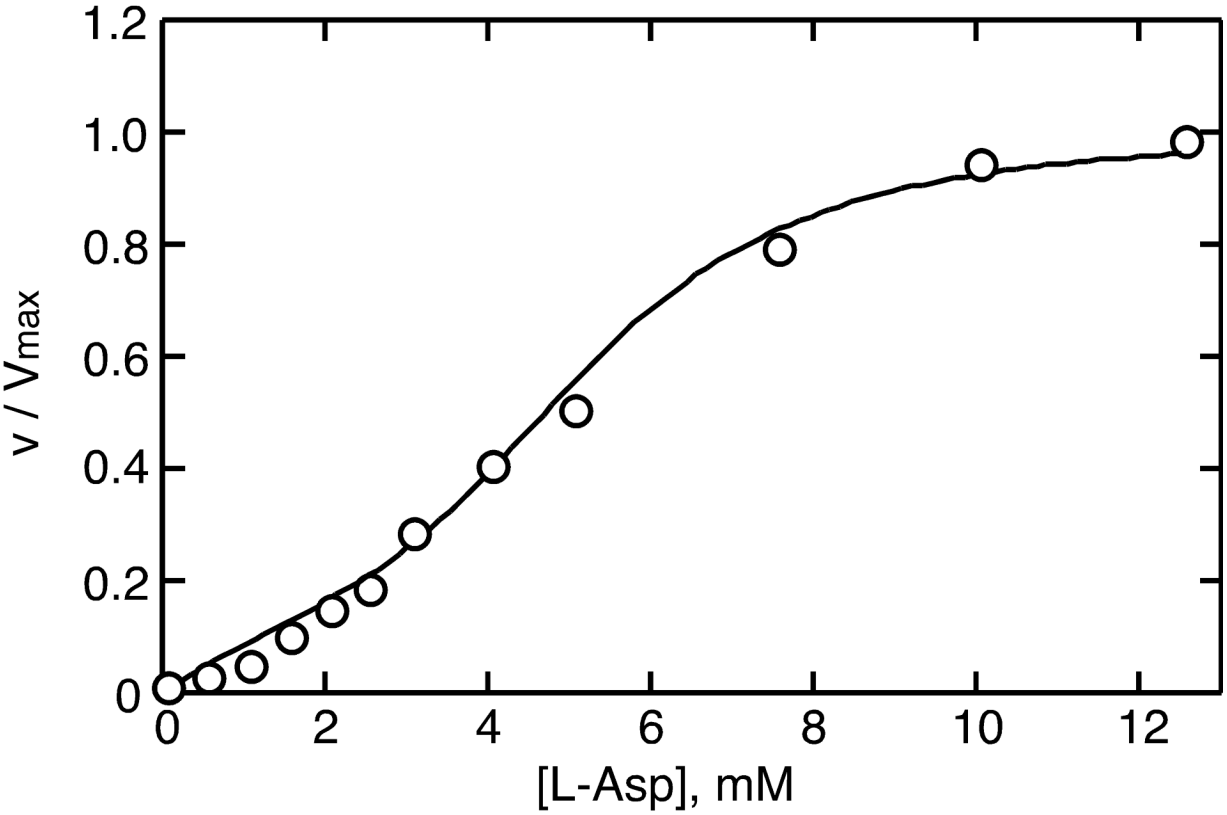

Figure 3.
L-Asp saturation kinetics at 5° C fitted by a theoretical curve calculated from a modified Monod *et al*. equation and using parameters listed in the text. Reactions were carried out in 50 mM Tris buffer, pH 8.3.

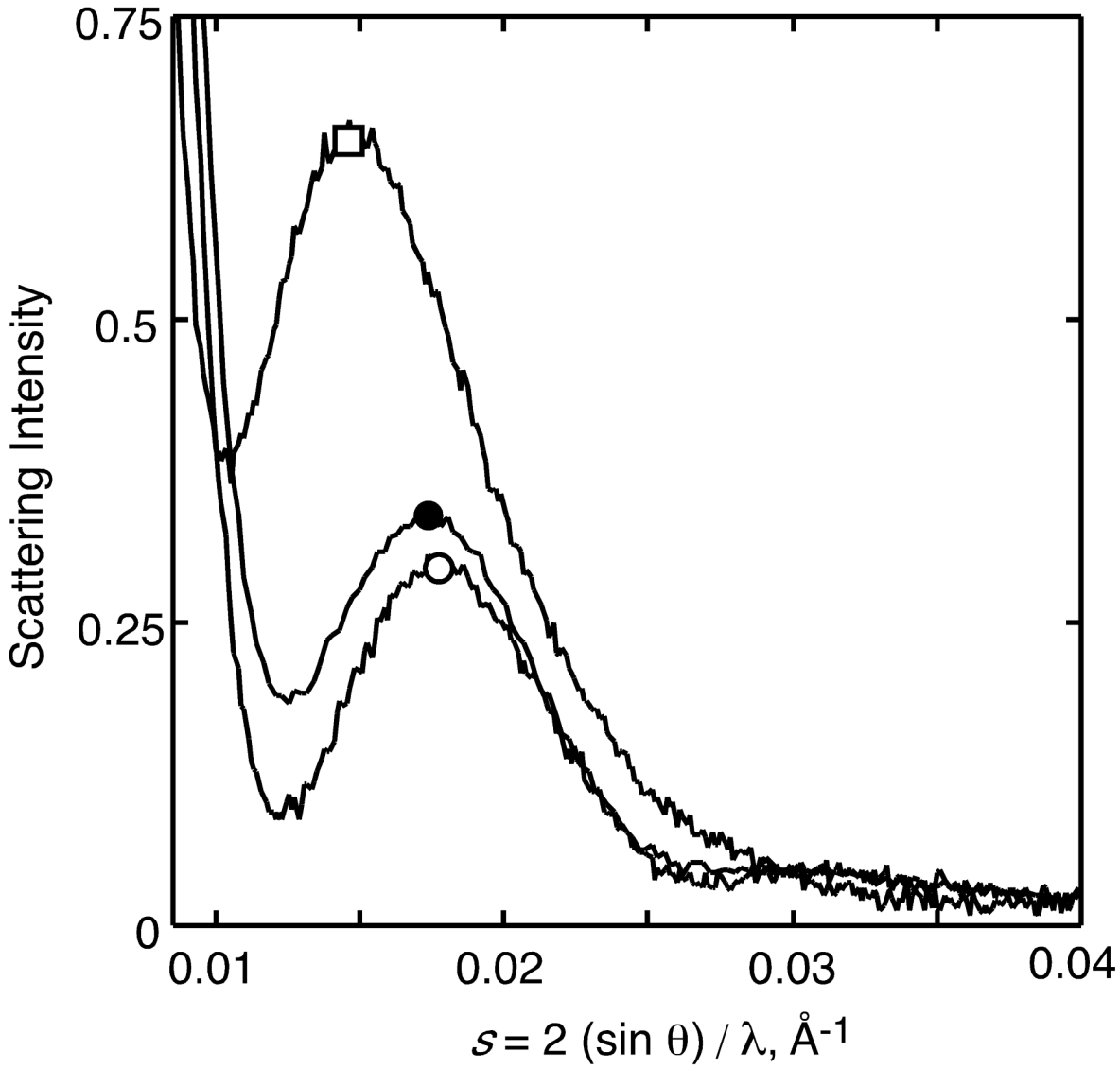

Figure 4.
Steady-state SAXS patterns of ATCase without ligands (○), with 50mM CP (●), and with 5mM PALA (□). The allosteric equilibrium constant was calculated from these curves as L' = 10.

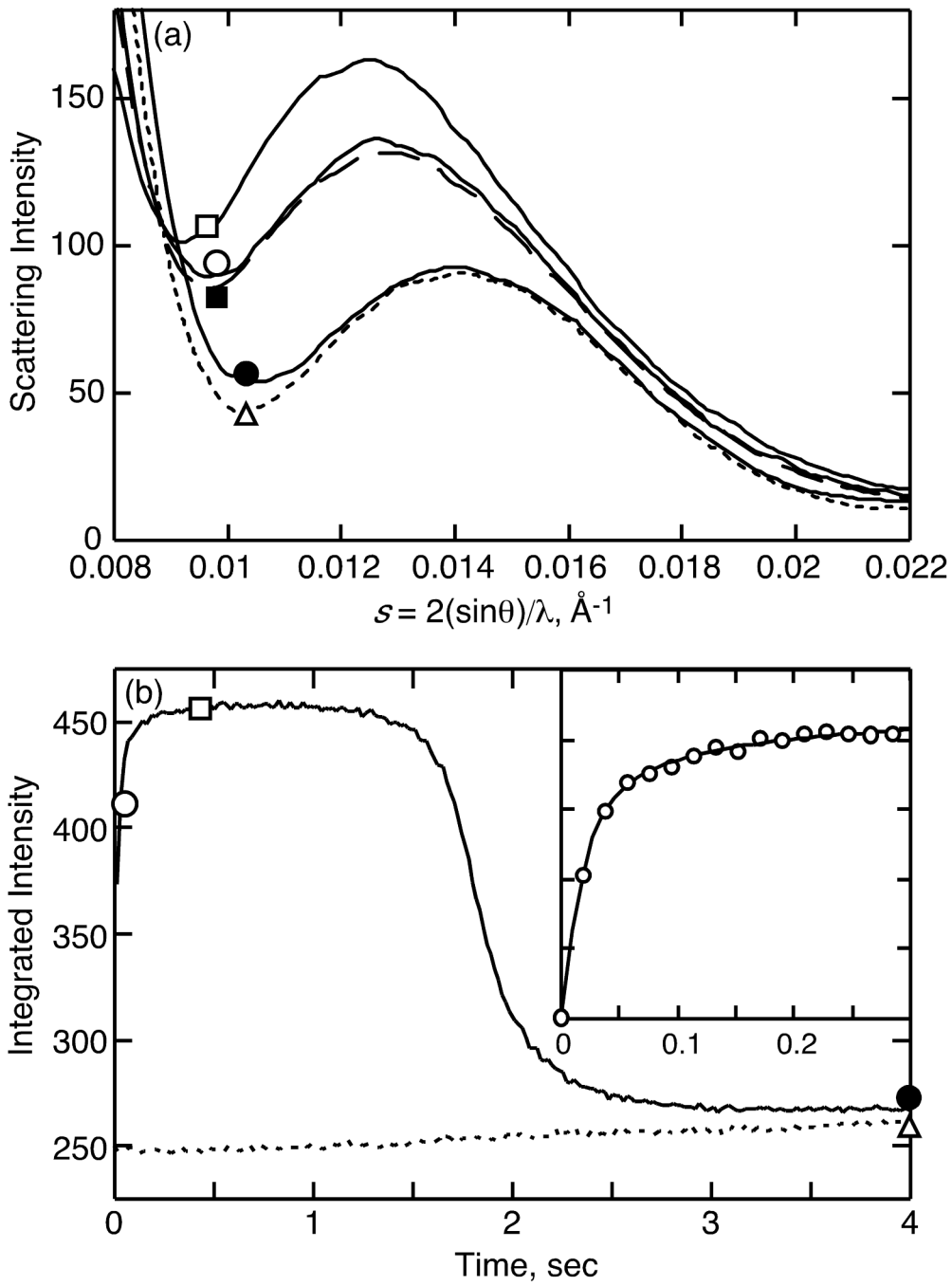

Figure 5.

(a) A time series of SAXS patterns of 0.75 mM ATCase (in active sites) mixed with 50 mM substrates (CP and L-Asp), and 50 mM CP plus 50 mM D-Asp as a T state control, at 5 °C. The SAXS patterns of the enzyme with the substrates are shown for 38 ms (○), 380 ms (□), and 3800 ms (●) after mixing. The SAXS pattern of the enzyme with CP and D-asp is shown for 3800 ms (Δ, short dashed curve) after mixing. The long dashed curve (■) is calculated for an L = 0.5, from the sum of 0.33 × (T state curve) and 0.67 × (R state curve). (b) Time-courses of the quaternary structure change after mixing with substrates (solid line) and 50 mM CP plus 50 mM D-Asp (short dashed line), as monitored by the scattering intensity integrated over the

s-range 0.085–0.152 $Å^{-1}$. Inset: First 300 ms of the structural change after mixing with substrates shown along with the curve fit (two exponential) to the data.

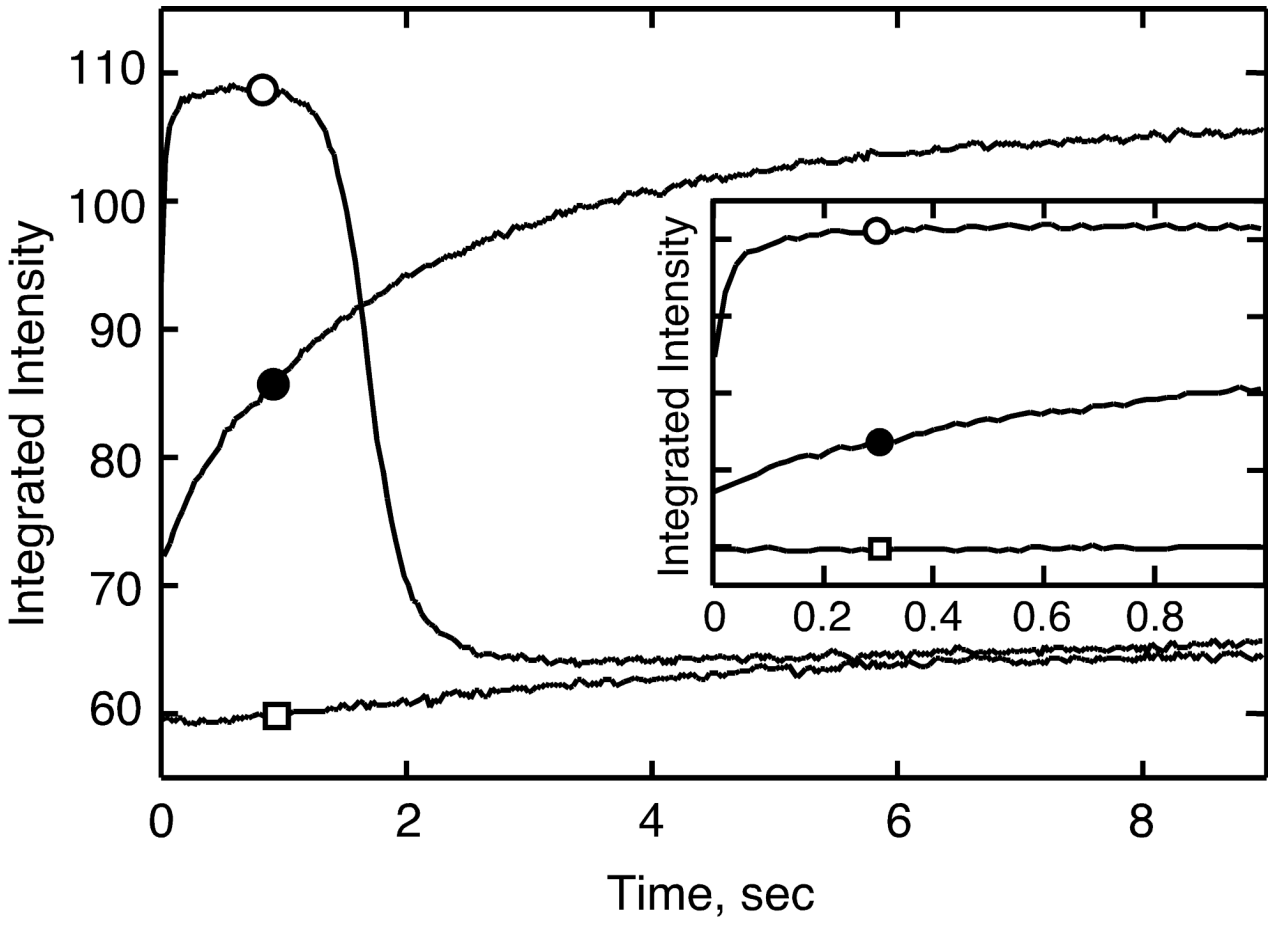

Figure 6.

Time-course of the quaternary structure change of 0.75 mM ATCase (in active sites) as monitored by the scattering intensity integrated over the *s*-range 0.085–0.152 $Å^{-1}$. The final substrate or substrate analog concentrations after mixing were [CP] = [*L*-Asp] = 50 mM (○), [CP] = 50 mM and [PALA] = 5 mM (●), and [CP] = [D-Asp] = 50 mM (□). Data displayed are from a 36 ms collection rate. Inset: First 1000 ms of the structural change after mixing with substrates or substrate analogs. Data displayed are from a 19 ms collection rate.

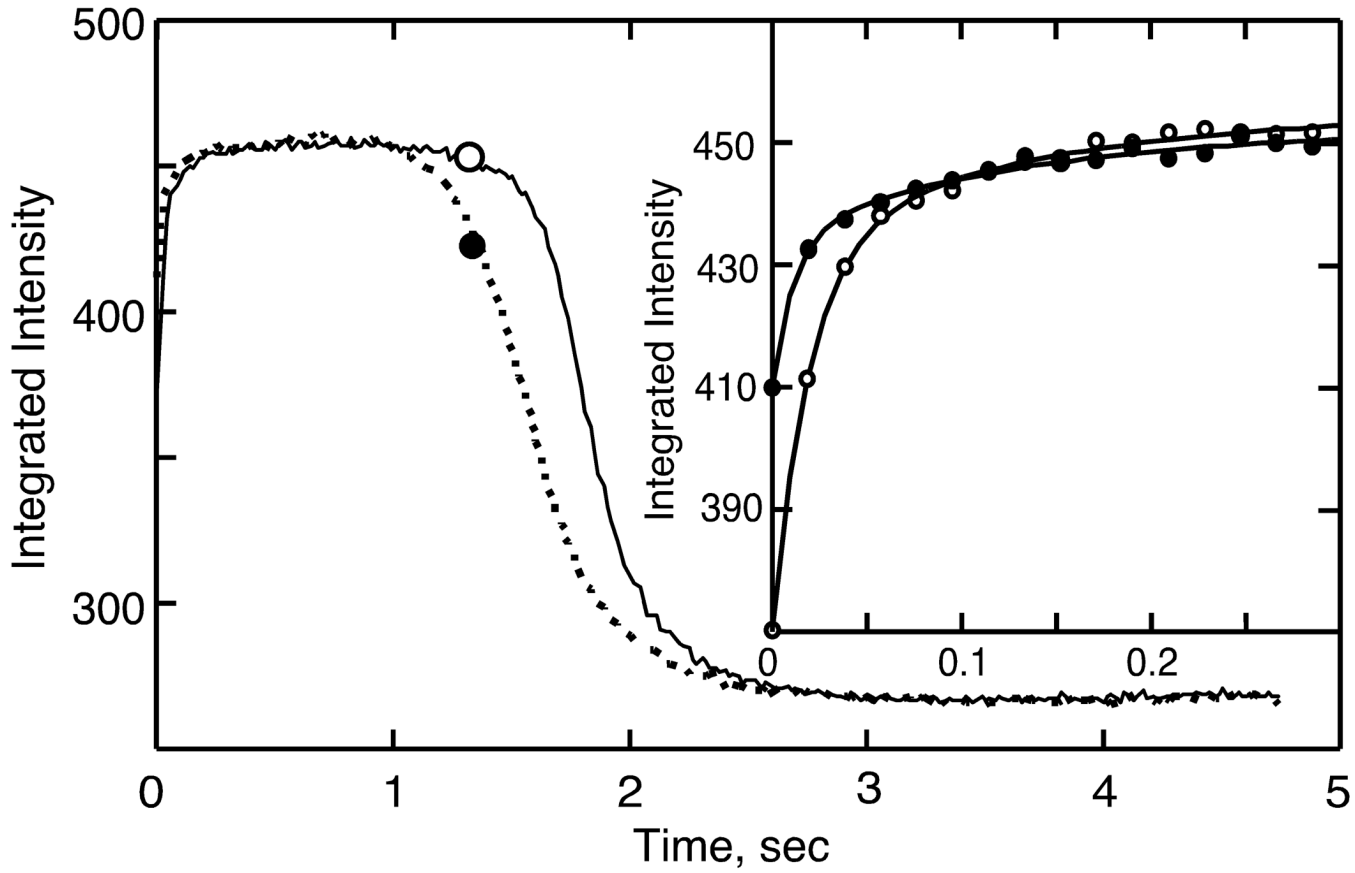

Figure 7.
Time evolution of the quaternary structure change of 0.75 mM ATCase (in active sites) as monitored by the scattering intensity integrated over the *s*-range 0.085–0.152 $Å^{-1}$ after mixing with 50 mM substrates (Asp and CP) and without nucleotides (○) and with [ATP] = 5 mM (●). Inset: First 300 ms of the structural change after mixing with substrates shown along with the curve fits (two exponential) to the data.

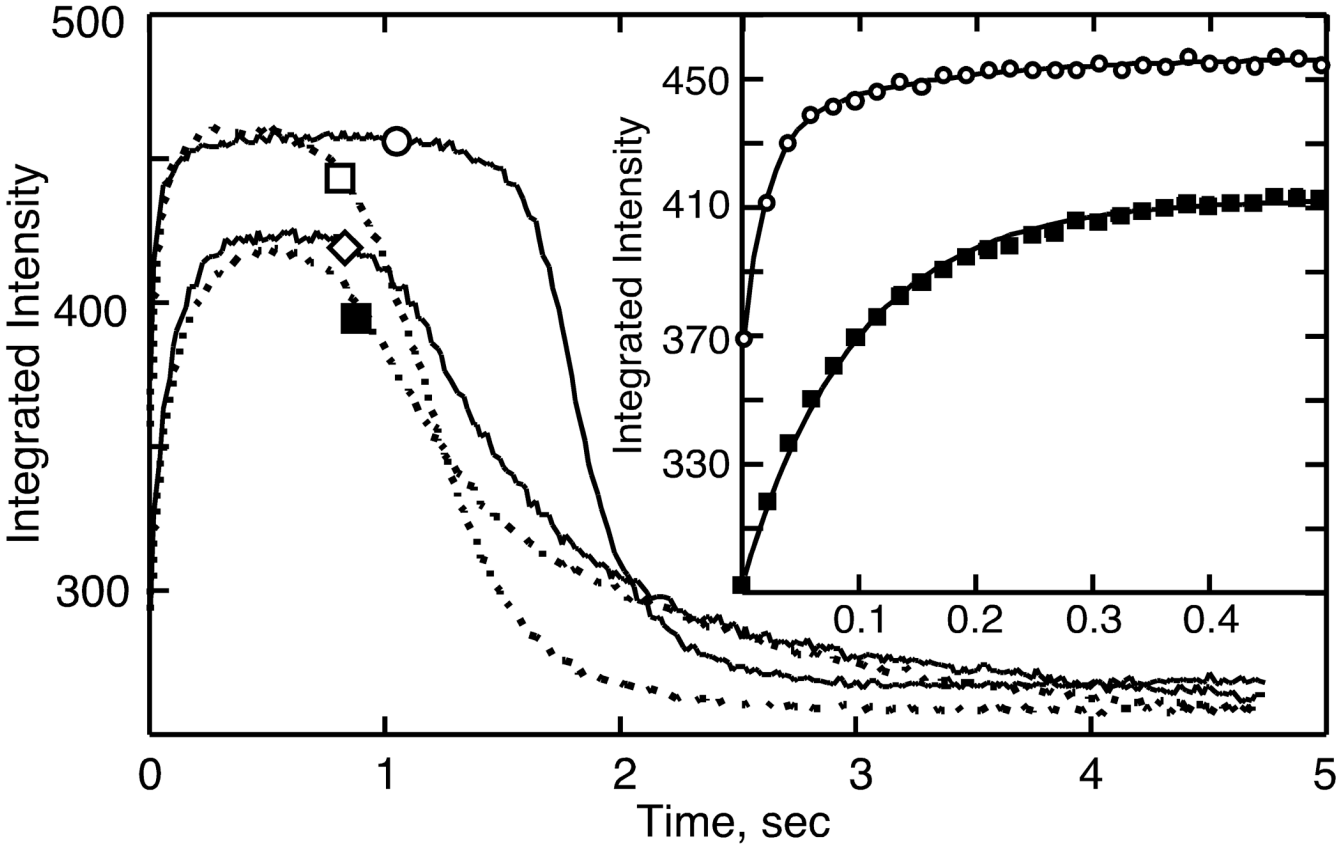

Figure 8.

Time evolution of the quaternary structure change of 0.75 mM ATCase (in active sites) as monitored by the scattering intensity integrated over the *s*-range 0.085–0.152 $Å^{-1}$ after mixing with 50 mM substrates (Asp and CP) and without nucleotides (○), with [CTP] = 4 mM (◊), with [UTP] = 4 mM (□, dashed curve), and with [CTP] = [UTP] = 4 mM (■, dashed curve). Inset: First 500ms of the structural change shown after mixing with substrates along with the curve fits to the data for without nucleotides (○,two exponential) and with CTP and UTP (■, one exponential).

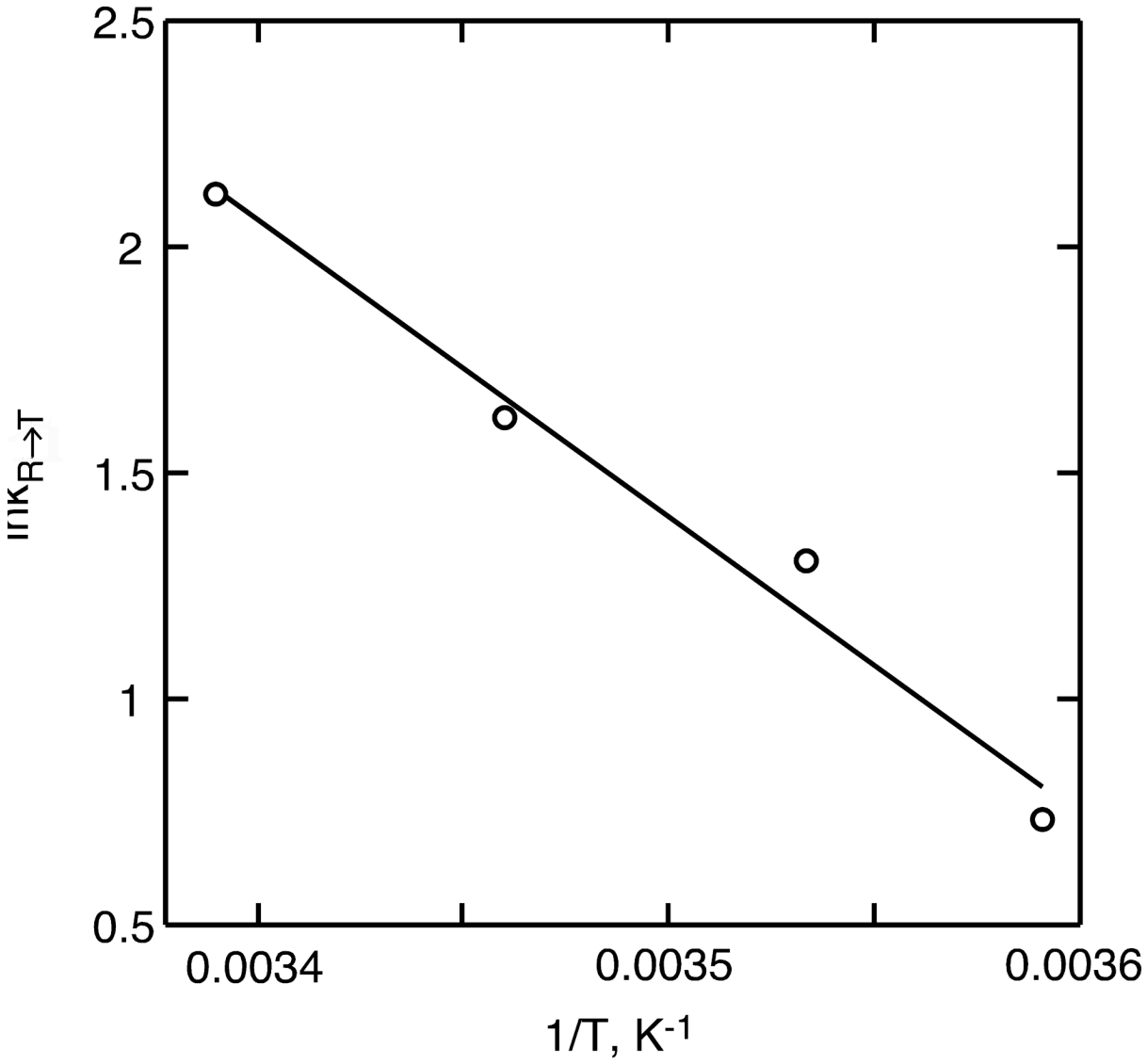

Figure 9.
Arrhenius plot of the temperature dependence of the R → T transition. The rate constants for the R to T transition ($k_{R\rightarrow T}$) at 5, 10, 16, and 22 °C were 2.08 ± 0.03, 3.7 ± 0.1, 5.1 ± 0.1, and 8.3 ± 0.1 s^{-1}, respectively.

Table 1

Kinetic parameters of ATCase with nucleotide effectors at 25 and 5 °C

Conditions[a]	V_{max}[b]	$[Asp]_{0.5}$[c] **25 °C**	n_H[d]	V_{max}[b]	$[Asp]_{0.5}$[c] **5 °C**	n_H[d]
No NTPs	19.1 ± 0.3	12.7	2.6 ± 0.2	4.2 ± 0.5	5.1	2.0 ± 0.1
5mM ATP	19.8 ± 0.7	6.1	1.4 ± 0.1	5.4 ± 0.2	2.9	1.6 ± 0.2
4mM CTP	17.9 ± 0.9	21.2	2.4 ± 0.1	3.6 ± 0.2	11.3	3.0± 0.1
4mM UTP	18.4 ± 0.2	13.5	2.3 ± 0.1	4.1 ± 0.6	5.9	2.2 ± 0.1
4mM CTP/UTP	17.3 ± 0.4	28.6	2.9 ± 0.1	3.0 ± 0.4	12.5	3.0 ± 0.1

[a] All experiments were performed in 50 mM Tris-acetate buffer (pH 8.3) at a saturating CP concentration (4.8 mM)

[b] The maximal observed velocity ($mmol \cdot h^{-1} \cdot mg^{-1}$)

[c] The observed concentration of L-Asp (mM) which produces one-half the observed maximal velocity

[d] Hill coefficient

Table 2

Kinetic parameters for the T to R allosteric transition of ATCase at 5 °C

Conditions[a]	$k_{T\rightarrow R1}$[b] (s^{-1})	$k_{T\rightarrow R2}$[c] (s^{-1})
25 mM substrates[d]	18.3 ± 0.6	
50 mM substrates	51 ± 4	7.6 ± 1
100 mM substrates	51 ± 5	6.3 ± 0.9
50 mM substrates + 5 mM ATP	89 ± 20	7.9 ± 1
50 mM substrates + 4 mM UTP	52 ± 8	14.8 ± 1.8
50 mM substrates + 4 mM CTP	12 ± 0.3	
50 mM substrates + 4 mM CTP / 4 mM UTP	10.3 ± 0.3	
50 mM succinate + 50 mM CP	38 ± 1	
5 mM PALA + 50 mM CP	1.53 ± 0.19	0.31 ± 0.05

[a] These experiments were performed in 50 mM Tris acetate buffer (pH 8.3), final enzyme concentration of 37.5 mg/ml after mixing, equal concentrations of substrates ([L-Asp] = [CP]) unless otherwise stated, and data points recorded at 19ms intervals

[b] Rate constant of fast phase or first phase of two-exponential fit

[c] Rate constant of slow phase or second phase of two-exponential fit, where applicable

[d] Final enzyme concentration used was 18.75 mg/ml because at this low substrate concentration (and a relatively high enzyme concentration) the substrates were exhausted before the enzyme fully attained the R state